

Metabolic consequences of susceptibility and resistance (race-specific and broad-spectrum) in barley leaves challenged with powdery mildew

PHILIP J. SWARBRICK¹, PAUL SCHULZE-LEFERT² & JULIE D. SCHOLES¹

¹Department of Animal and Plant Sciences, University of Sheffield, Western Bank, Sheffield, S10 2TN, UK and ²Department of Plant Microbe Interactions, Max Planck Institute for Plant Breeding Research, Cologne D-50829, Germany

ABSTRACT

In a compatible interaction biotrophic fungi often lower the yield of their hosts by reducing photosynthesis and altering the fluxes of carbon within the infected leaf. In contrast, comparatively little is known about the metabolic consequences of activating resistance responses. In this study we investigated the hypothesis that the activation of both race-specific (*Mla12*) and broad-spectrum (*mlo*) resistance pathways in barley leaves infected with *Blumeria graminis* represents a cost to the plant in terms of carbon production and utilization. We have shown, using quantitative imaging of chlorophyll fluorescence, that during a susceptible interaction, photosynthesis was progressively reduced both in cells directly below fungal colonies and in adjacent cells when compared with uninoculated leaves. The lower rate of photosynthesis was associated with an increase in invertase activity, an accumulation of hexoses and a down-regulation of photosynthetic gene expression. During both *Mla12*- and *mlo*-mediated resistance, photosynthesis was also reduced, most severely inhibited in cells directly associated with attempted penetration of the fungus but also in surrounding cells. These cells displayed intense autofluorescence under ultraviolet illumination indicative of the accumulation of phenolic compounds and/or callose deposition. The depression in photosynthesis was not due only to cell death but also to an alteration in source-sink relations and carbon utilization. Apoplastic (cell wall-bound) invertase activity increased more rapidly and to a much greater extent than in infected susceptible leaves and was accompanied by an accumulation of hexoses that was localized to areas of the leaf actively exhibiting resistance responses. The accumulation of hexoses was accompanied by a down-regulation in the expression of Rubisco (*rbcS*) and chlorophyll a/b binding protein (*cab*) genes (although to a lesser extent than in a compatible interaction) and with an up-regulation in the expression of the pathogenesis-related protein 1 (*PR-1*). These results are consistent with a role for invertase in the

generation of hexoses, which may supply energy for defence reactions and/or act as signals inducing defence gene expression.

Key-words: *Blumeria graminis*; *Hordeum vulgare*; chlorophyll fluorescence imaging; invertase; photosynthesis; resistance; sugar metabolism.

INTRODUCTION

Biotrophic fungi are agriculturally destructive pathogens that can cause severe losses in crop yield. During a compatible interaction, photosynthesis is often reduced in comparison to an uninfected plant (Farrar & Lewis 1987; Scholes 1992; Ayres, Press & Spencer-Phillips 1996). However, as infected leaves are heterogeneous consisting of regions of cells directly invaded by the pathogen and regions remote from the fungal colony, alterations in photosynthesis are often spatially and temporally complex and depend upon the particular host/pathogen interaction (e.g. Scholes & Rolfe 1996; Osmond *et al.* 1998; Chou *et al.* 2000). The heterogeneity in the rate of photosynthesis within infected leaves is likely to be a consequence of pathogen-induced alterations in source-sink relationships. Many studies have shown that a key event in a compatible interaction is a pathogen-induced stimulation of host apoplastic (cell wall-bound) invertase activity leading to an accumulation and/or alteration in fluxes of hexose sugars and, in some cases, to a reduction in export of sucrose from the leaf. The localized accumulation of soluble sugars is thought to favour pathogen nutrition and may also be responsible, via the triggering of one or more sugar-signal transduction pathways, for the down-regulation of photosynthetic gene expression observed in these leaves (Scholes *et al.* 1994; Tang, Rolfe & Scholes 1996a; Chou *et al.* 2000; Fotopoulos *et al.* 2003; Berger *et al.* 2004).

Although the changes in host physiology associated with compatible interactions are well characterized, less is known about the effects of incompatible plant–pathogen interactions on host photosynthesis and carbon metabolism, despite the fact that the activation of resistance responses can lead to a reduction in crop yield when com-

Correspondence: Julie Scholes. Fax: +44 114 22 20002; e-mail: J.Scholes@Sheffield.ac.uk

pared to unchallenged plants (Smedegaard-Petersen & Tolstrup 1985; Purrington 2000; Brown 2002; Tian *et al.* 2003). Upon recognition of an invading pathogen, a range of defence mechanisms may be triggered to restrict its growth including the production of reactive oxygen species, the death of host cells in a hypersensitive response (HR) or the induction of pathogenesis-related (PR) proteins (Hammond-Kosack & Jones 1996). An increase in invertase activity has also been reported in roots or leaves undergoing resistance reactions (Benhamou, Grenier & Chrispeels 1991; Heisterüber, Schulte & Moerschbacher 1994) and it has been suggested that this enzyme should be considered a PR protein (Sturm & Chrispeels 1990; Roitsch *et al.* 2003). Although the significance of the increase in invertase activity is not fully understood, the localized production of hexoses may be crucial to supply extra energy required for the activation of defence responses.

In a compatible interaction *Blumeria graminis* f. sp. *hordei* produces extensive mycelial growth on the surface of barley leaves and forms haustoria in epidermal cells, through which it obtains water and nutrients. Resistance to this pathogen can be triggered by a large number of race-specific resistance genes, usually dominant alleles at loci designated *Mlx*, for example, *Mla12* (Jorgensen 1994). Resistance controlled by *Mla12* is tightly associated with the death of the penetrated epidermal cells and this cell-death response then consumes subtending mesophyll tissue (Hückelhoven *et al.* 1999). Recessive mutations in the barley *Mlo* gene give rise to broad-spectrum (*mlo*) resistance to all tested races of the barley-powdery mildew pathogen (Jorgensen 1992; Büschges *et al.* 1997). Resistance due to *mlo* occurs during attempted entry into epidermal cells and is associated with the formation of a cell-wall apposition beneath a fungal appressorium (Wolter *et al.* 1993). Although growth of *B. graminis* is halted during penetration of an epidermal cell without an accompanying cell-death response, small numbers of subtending mesophyll cells undergo cell death at a later stage (Shirasu & Schulze-Lefert 2000; Piffanelli *et al.* 2002).

In this study, we used near-isogenic backcross lines of barley (cultivar Ingrid) which were either susceptible or exhibited *Mla12* or *mlo* resistance to the same isolate of *B. graminis* to investigate the hypothesis that the activation of resistance pathways represents a cost to the plant by altering both the rate of photosynthesis and carbon metabolism. Specifically, we aim to: (1) quantify and localize alterations in photosynthesis in leaves undergoing susceptible (compatible) and resistant (incompatible) interactions, using high-resolution chlorophyll fluorescence imaging; (2) quantify changes in the activity of apoplastic and soluble (vacuolar) acid invertases and the amounts of soluble carbohydrates in infected leaves; and (3) examine temporal changes in the expression of genes encoding photosynthetic proteins Rubisco (*rbcS*) and chlorophyll *a/b* binding protein (*cab*), and defence-related proteins pathogenesis-related protein 1 (*PR-1*), phenylalanine ammonia lyase (*PAL*) and peroxidase.

MATERIALS AND METHODS

Plant growth and inoculation

Seeds of the barley (*Hordeum vulgare* L.) cultivar Ingrid (*Mlo*, *mLa12*; compatible), the near-isogenic backcross lines BCIngrid-*Mla12* (*Mlo*, *Mla12*; race-specific resistant) and BCIngrid-*mlo5* (*mlo*, *mLa12*; broad-spectrum resistant) were pre-germinated for 24 h in water and sown in Levington M3 compost (Scotts UK professional, Ipswich, UK). The plants were grown in controlled-environment cabinets (Fisons Fi-totron 600H, Sanyo Gallenkamp, Leicester, UK) under a 16 h photoperiod at an irradiance of $230 \mu\text{mol m}^{-2} \text{s}^{-1}$, supplied by fluorescent lamps (OSRAM L 58W/77 Fluora, Munich, Germany). Temperatures were maintained at 21 °C by day and 19 °C by night in 60 and 80% relative humidity, respectively. Eight days after germination, the seedlings were inoculated with *B. graminis* f. sp. *hordei* race A6 (*AvrMla12*), which had been maintained on compatible plants. A spore suspension of 10^5 mL^{-1} was prepared in Fluorinert (Sigma-Aldrich, Poole, Dorset, UK), which was sprayed onto the adaxial surface of the first fully expanded leaf (primary leaf) using an airbrush (Badger, Franklin Park, IL, USA). The density of spores was approximately 20 per mm^2 . Control plants were sprayed with Fluorinert and treated in an identical manner. In an experiment to measure sugar content and invertase activity in infected and uninfected regions of the same leaf, primary leaves of 10-d-old barley plants were infected while gently secured to a horizontal surface, with the adaxial side upwards. The plant was covered by a plastic sheet leaving only 3 cm towards the leaf tip exposed to inoculation with the spore suspension (or Fluorinert, in the case of control leaves) as described above.

Visualizing the development of symptoms and resistance responses

For comparison of macroscopic symptoms, images of leaves infected with *B. graminis* were captured at 3, 5 and 7 d after inoculation (DAI) using a colour charge-coupled device (CCD) camera (Photometrics Coolsnap, Roper Scientific, Marlow, Buckinghamshire, UK) mounted on a copy stand. Illumination was provided by a fibre optic lamp (Schott, Mainz, Germany) and reflection from the leaf surface was minimized by the use of standard polarizing filters (Jessop, Leicester, UK).

In order to visualize the development of fungal mycelium on infected leaves, leaf segments were harvested 5 DAI and cleared of chlorophyll by placing these abaxial surface-down overnight on cotton-wool pads moistened with ethanol:acetic acid (3:1). Leaf segments were then placed on water-soaked pads for 4 h to rehydrate the tissue, and finally onto pads moistened with lactoglycerol (1:1:1, lactic acid:glycerol:water) overnight. Mycelium on the leaf was stained for 10 s with 0.6% Brilliant Blue R (Sigma-Aldrich) in methanol, then rinsed with dH_2O and mounted in 50% glycerol. Cleared leaves were viewed

using an Olympus BX50WI fluorescence microscope (Olympus Optical Company, London, UK), with transmitted light provided by a tungsten-halogen light source (Olympus Optical Company). Images were acquired using a colour CCD camera.

To visualize autofluorescent material in inoculated plants 24 and 36 h after inoculation, leaves (still attached to the plants) were secured to the stage of a fluorescence microscope, using magnetic strips. Leaves were irradiated with light provided by a Xenon Arc lamp EBX 75. Light was passed through a U-MWBV filter cube (Olympus) providing excitation irradiance of 400 to 440 nm. Fluorescence from the sample was detected at wavelengths between 475 and 600 nm. This was achieved by a combination of a dichroic mirror and emission filter in the filter cube and by an additional short-pass filter (600 nm; Olympus) to exclude chlorophyll fluorescence. Images were captured using a colour CCD camera.

CO₂ assimilation and chlorophyll fluorescence imaging

Imaging of chlorophyll fluorescence and the simultaneous measurement of CO₂ assimilation was performed essentially as described by Rolfe & Scholes (1995). The 3, 5 and 7 DAI barley plants were removed from the growth cabinets and a leaf (still attached to the plant) was immediately placed in the chamber of an IRGA (LCA-4 with PLCA4 leaf chamber; Analytical Development Company, Hoddesdon, Herts, UK). The CO₂ concentration was maintained at 340 $\mu\text{mol mol}^{-1}$ with 60% relative humidity. CO₂ assimilation was recorded every 30 s during the experiment. Chlorophyll fluorescence images were captured using a monochrome CCD camera (4722-2000/0000, Cohu, San Diego, CA, USA) with a filter of peak transmission 694.3 nm (Ealing-Optics, Watford, UK). The leaf was initially kept in the dark for 5 min and a rate of respiration measured. In addition, an image was captured during darkness to represent zero fluorescence. The leaf was then exposed to 2 $\mu\text{mol m}^{-2} \text{s}^{-1}$ actinic irradiance, provided by fibre-optic lamps, and an image of minimal chlorophyll fluorescence (F_0) was captured. Immediately after, the leaf was given a pulse of saturating irradiance ($\sim 3000 \mu\text{mol m}^{-2} \text{s}^{-1}$) lasting 1.5 s at the end of which an image of maximal chlorophyll fluorescence (F_m) was captured. Thirty seconds later, the leaf was irradiated with actinic light of 80 $\mu\text{mol m}^{-2} \text{s}^{-1}$. The leaf was exposed to a pulse of saturating illumination 10 and 50 s after the commencement of actinic illumination and subsequently every 60 s. Two images were captured at each pulse: one just before (F_s) and one at the peak (F_m') of each flash. After 15 min photosynthesis had reached a steady-state value and the actinic irradiance was increased to 200 $\mu\text{mol m}^{-2} \text{s}^{-1}$ for a further 10 min, during which images of chlorophyll fluorescence were captured every 60 s for the last 4 min. Four replicate leaves from each interaction (control, *mlo* resistance, *Mla12* resistance and susceptible leaves) were imaged at each time-point.

Fine resolution chlorophyll fluorescence imaging

At 3 DAI, the number of cells affected by fungal penetration (or attempted penetration) was small. In order to determine the effects of these early events on photosynthesis, chlorophyll fluorescence images were obtained using a microscope-based, high-resolution imaging system as described by Rolfe & Scholes (2002). Leaves, still attached to the plant, were carefully secured to the stage of a modified Olympus BX50WI microscope. Leaves were kept in the dark for 10 min and then exposed to 5 $\mu\text{mol m}^{-2} \text{s}^{-1}$ blue light (420–480 nm) for 3 min. This irradiance did not quench chlorophyll fluorescence but triggered chloroplasts to move and settle, thus avoiding large-scale movement during the experiment. The leaf was then exposed to an actinic irradiance (350–620 nm) of 2 $\mu\text{mol m}^{-2} \text{s}^{-1}$ and a F_0 image was captured using a monochrome CCD camera (Micromax 800PB, Roper Scientific). The leaf was then exposed to a saturating flash of 3000 $\mu\text{mol m}^{-2} \text{s}^{-1}$ of 1.5 s duration, at the end of which an F_m image was captured. Leaves were then illuminated with an irradiance of 80 $\mu\text{mol m}^{-2} \text{s}^{-1}$ to allow photosynthesis to reach a steady-state value. Next the actinic irradiance was increased to 200 $\mu\text{mol m}^{-2} \text{s}^{-1}$ and images were captured after 6 min and every 60 s for 4 min. A fluorescence standard was used to accurately determine the relative irradiances for each set of acquisition conditions and to correct for alterations in exposure required to capture on-scale images of variable fluorescence intensity (Rolfe & Scholes 2002). All aspects of image acquisition were computer-controlled using custom software developed at the University of Sheffield. After the chlorophyll fluorescence images had been acquired, ultraviolet (UV) autofluorescence images were also captured as described previously except using a Micromax 800PB CCD camera. Four replicate leaves from each interaction (control, *mlo* resistance, *Mla12* resistance and susceptible leaves) were imaged.

Calculation of chlorophyll fluorescence parameters

Image analysis was carried out using Image-Pro Plus version 4.1 (Media Cybernetics, Wokingham, Berkshire, UK). Images of chlorophyll fluorescence were used to calculate images of the following: the proportion of light energy flowing through photosystem II (ΦPSII) [$(F_m' - F_s)/F_m'$], the rate of electron transport (ETR) [$\Phi\text{PSII} \times \text{absorbed irradiance} \times 0.5$] and a measure of non-photochemical quenching (NPQ) [$(F_m - F_m')/F_m'$] according to Rolfe & Scholes (1995, 2002). To calculate the amount of light absorbed by a leaf, images were captured following exposure to red (R) and then near infrared (NIR) irradiance. The apparent absorptivity was calculated pixel by pixel from the R and NIR images using the formula $\text{Absorbance} = 1 - \text{R/NIR}$, as developed for the Imaging-Pam Chlorophyll Fluorimeter (Heinz-Walz GmbH, Effeltrich, Germany).

Values of Φ PSII, ETR and NPQ were extracted from images of control and infected leaves 3, 5 and 7 DAI in order to quantify and compare the heterogeneity within infected leaves. Values were extracted from the centre of the fungal colony in a susceptible interaction or the area of cells undergoing a resistance reaction, the regions immediately adjacent to the lesion/colony and the regions remote from (> 3 mm) the lesion/colony. Values from areas of similar size were extracted from control leaves for comparison. All areas were manually defined from raw chlorophyll fluorescence (F_m) images and an average value for each area was calculated.

An integrated ETR for an average-sized barley leaf was calculated from Φ PSII images obtained during steady-state photosynthesis at $200 \mu\text{mol m}^{-2} \text{s}^{-1}$ irradiance, 7 DAI. The different regions of each leaf segment (centre of lesion/colony, adjacent to lesion/colony and the remainder of the leaf) were defined using a threshold function. A binary image (or mask) of each of the areas was then made. Subtracting each mask from the original Φ PSII image produced individual Φ PSII images for each of the regions. The mean value of Φ PSII (weighted for area) and the total area occupied by the particular region was then extracted using a custom-written macro in Image-Pro Plus. An integrated whole-leaf ETR ($\text{nmol } 10 \text{ cm}^{-2} \text{ leaf s}^{-1}$) and the percentage of the whole-leaf ETR contributed by each region were then calculated.

Measurement of soluble carbohydrates and invertase activity

In order to determine the impact of *B. graminis* on the soluble carbohydrate content and invertase activity of leaves during the susceptible and resistant interactions, 3 cm^2 leaf segments were harvested from four control or infected plants 6 h into the photoperiod 0, 1, 2, 3, 5 and 7 DAI. To calculate the diurnal turnover of soluble carbohydrates, leaf segments were also collected immediately prior to and 10 h after the onset of the photoperiod 3, 5 and 7 DAI. To determine whether changes in soluble carbohydrate content and invertase activity were localized to areas directly affected by fungal colonization (or areas undergoing a defence response), small areas (2 cm^2) were harvested from infected and uninfected regions of leaves infected only at the apical 3 cm, and from comparable areas of a control leaf 3 and 5 DAI. After harvesting, samples were immediately frozen in liquid N_2 .

Sucrose, glucose and fructose were extracted and measured as described by Scholes *et al.* (1994). To measure soluble and apoplastic acid invertase activities, the leaf samples were homogenized in 2 mL microtubes containing a ball bearing and $750 \mu\text{L}$ cold-extraction buffer (20 mM sodium phosphate buffer with pH of 6.5, 1 mM ethylenediaminetetraacetic acid (EDTA), 1 mM dithiothreitol [DTT], 1 mM benzamidine and 1 mM phenylmethylsulfonyl fluoride) for 10 min at 4°C using an 8000 M Mixer/Mill grinding machine (Glen Creston Ltd, Stanmore, Middlesex, UK). After centrifugation at $14\,000 \times g$ at 4°C for 10 min, the

supernatant (containing soluble invertase activity) was removed. The pellet was washed by resuspending in $750 \mu\text{L}$ cold-extraction buffer and repeated in a $750 \mu\text{L}$ cold extraction buffer containing 50 mM NaCl to remove sugars and residual soluble invertase activity. Invertase activities were assayed as described by Tang *et al.* (1996b).

Measurement of sucrose synthase activity

For measurement of sucrose synthase (SS) activity, 4 cm^2 leaf segments were collected 6 h into the photoperiod 3, 5 and 7 DAI. Leaves were homogenized as described above, in a $750 \mu\text{L}$ cold-extraction buffer (50.0 mM Hepes KOH with pH of 7.4, 5.0 mM MgCl_2 , 1.0 mM EDTA, 1.0 mM ethylene glycol bis-2-aminoethyl ether-n,n',n'',n'-tetraacetic acid [EGTA], 1.0 mM DTT, 2.0 mM Benzamidine, 0.5 mM PMSF and 0.1% [v/v] Triton X-100). Extracts were then centrifuged at $12\,000 \times g$ at 4°C for 5 min and the supernatants were immediately assayed for enzyme activity using a modified version of the Dancer, Hatzfeld & Stitt (1990) method. Extracts were incubated for 30 min at 25°C in assay medium containing 20 mM Hepes-KOH (pH 7), 100 mM sucrose and 4 mM uridine 5'-diphosphate (UDP). To account for endogenous UDP in extracts, blank incubations were also performed in the absence of UDP. Reactions were halted by boiling for 4 min. The amount of UDP-glucose generated was measured in an assay containing UDP-glucose dehydrogenase (0.02 U) in 200 mM glycine (pH 8.9), 5 mM MgCl_2 and 2 mM NAD^+ . The generation of NADH due to the action UDP-glucose dehydrogenase was detected spectrophotometrically at 340 nm.

Quantification of gene expression by real-time PCR

Leaf tissue of 100 mg was harvested from infected and uninfected barley leaves 0, 1, 2, 3, 5 and 7 DAI with *B. graminis*, 6 h into the photoperiod. RNA isolation was carried out using RNAwiz (Ambion, Huntingdon, Cambridgeshire, UK) according to the manufacturer's instructions. RNA was quantified using a UV-2101PC, UV-VIS Scanning Spectrophotometer (Shimadzu, Kyoto, Japan) at a wavelength of 260 nm.

In order to remove any residual genomic DNA, RNA samples were treated with DNase I (Ambion) according to the manufacturer's instructions. RNA samples were then subjected to PCR using primers for a putative actin gene (see Table 1) to verify that there was no DNA contamination. PCR reactions were carried out using a Techne PCR machine (Scientific Laboratory Supplies, Nottingham, UK) in a reaction containing 5 units *Taq* polymerase (Promega, Madison, WI, USA), 10.0 mM Tris-HCl with pH of 9, 50.0 mM KCl, 0.1% Triton X-100, 1.5 mM MgCl_2 , 0.2 mM deoxynucleotide triphosphate (dNTP), $4.0 \mu\text{M}$ forward primer and $4.0 \mu\text{M}$ reverse primer. Reaction conditions were 95°C for 5 min, followed by 35 cycles at 95, 55 and 72°C for 30 s, 60 s and 2 min, respectively, and finally 72°C for 6 min. Following PCR, each sample was mixed with 5x

Table 1. Gene accession numbers/references and oligonucleotide primer sequences used in quantitative RT PCR experiments

Gene	GenBank accession # (TIGR EST #)	Gene reference	Sequence of forward and reverse oligonucleotides, respectively (amplicon size in parentheses)
Actin	BI953579 (TC98292) ^a	–	5'-ACACTCCTGCTATGTATGTC-3' 5'-ATCTCCGAGGTCCAGCACAA-3' (88)
<i>cab</i>	AJ006296	–	5'-GTATGACGAGTGATGGATGA-3' 5'-CAGCAGCTCTCCTATGTGAT-3' (82)
<i>PAL</i>	Z49145	Peltonen & Karjalainen (1995)	5'-GAGTACACCGACCACTTGAC-3' 5'-AGTATCATGTAGGAGCTACC-3' (103)
Peroxidase	AJ003141	Kristensen, Bloch & Rasmussen (1999)	5'-ATAACCAATCGGTGTAAC-3' 5'-TTGGCTAGACATCACACT-3' (104)
<i>PR-I</i>	Z21494	Muradov <i>et al.</i> (1993)	5'-CCAGAACTACGCCAACCA-3' 5'-TCCTTCTTCTCGCTCACC-3' (143)
18S-26S ribosomal intergenic region RNA	AF147501	–	5'-CGTGTACGACTCATGCCA-3' 5'-AGATCACATCGACCTGAC-3' (101)
<i>rbcS</i>	U43493	Lee, Parthier & Lobler (1996)	5'-TACTACGATGGCCGGTACTG-3' 5'-TTCTTGACCTTCCACCTC-3' (94)
Tubulin	U40042	–	5'-GTATCAACTACCACCACT-3' 5'-GGAGAAGACCTCAACAACAC-3' (106)

^aIn the case of the putative actin sequence, TIGR EST number is given in parentheses.

cab, chlorophyll *a/b*; *PAL*, phenylalanine ammonia lyase; *PR-I*, pathogenesis-related protein 1; *rbcS*, Rubisco.

gel-loading buffer (Sigma-Aldrich) and subjected to gel electrophoresis on a 2% (w/v) TAE-agarose gel (0.05 µg/mL ethidium bromide) to determine the size of any amplicons relative to DNA Hyperladder II (Bioline, London, UK). Gels were visualized on an Epi Chem II Darkroom gel-documentation system (UVP Laboratory products, Cambridge, UK). There was no DNA contamination of DNase treated RNA samples.

First strand cDNA was synthesized from 4 µg of RNA using SuperScript II Reverse Transcriptase (Invitrogen, Paisley, UK) according to the manufacturer's instructions, and subsequently purified using a PCR purification kit (Qiagen, Crawley, West Sussex, UK). Expression of genes encoding *rbcS*, *cab*, *PR-I*, *PAL* and peroxidase were quantified by quantitative RT PCR. To take account of small differences in cDNA input, the expression of each target gene was calculated relative to that of a reference gene, whose expression did not change in infected tissue when compared to control tissue during the experiment's duration. Three reference genes were used: tubulin, 18S–26S ribosomal intergenic region and a putative actin gene (an expressed sequence tag [EST] with >97% homology to actin sequences from oat, rice, *Arabidopsis thaliana* and tobacco; Table 1). The suitability of a target/reference gene combination was established by demonstrating a similar efficiency of amplification as described in User Bulletin #2 (ABI Prism 7700 Sequence Detection System, Applied Biosystems, Warrington, UK). Target/reference gene combinations were: *rbcS*/18S–26S ribosomal intergenic region RNA, *cab*/actin, *PR-I*/actin, *PAL*/actin and peroxidase/tubulin. All primers were designed against an EST sequence for each gene and are presented in Table 1. The primers were found to be selective, yielding only one amplicon of the predicted length following PCR of cDNA samples.

For quantitative amplification of cDNA, 25 µL reactions were prepared in a 96 Well optical reaction plate (Applied Biosystems), each reaction comprising 5.0 µL template cDNA, 12.5 µL 2x SYBR Green PCR Master Mix (Applied Biosystems) and 7.5 µL of a solution containing the forward and reverse primers for one gene (~12 pmoles of each primer per reaction). Amplification was performed using an ABI Prism 7700 Sequence Detector (Applied Biosystems) using the following cycling conditions: 50 and 95 °C for 2 and 10 min, respectively, followed by 40 cycles of 95 and 60 °C for 15 s and 1 min, respectively. The incorporation of a fluorescent marker (SYBR green) into amplicons was detected in real time, and the data were analysed using Sequence Detector version 1.7 software (Applied Biosystems). In order to quantify gene expression, the amount of target cDNA was calculated relative to that of a reference gene (to normalize for cDNA input), and the values were then expressed relative to the control leaf sample at 1 DAI using the equation:

$$\text{Relative expression} = 2^{-\Delta\Delta\text{CT}}$$

Where CT is the cycle at which fluorescence detection reached a threshold level (during the exponential amplification phase); ΔCT is the CT target gene–CT reference gene; $\Delta\Delta\text{CT}$ is the ΔCT sample– ΔCT 1 DAI control tissue (User Bulletin #2, ABI Prism 7700 Sequence Detection System, Applied Biosystems). Data presented are representative of two independent RT PCR experiments.

Statistical analyses

Data from gas exchange, steady-state chlorophyll fluorescence imaging, invertase activity, SS activity and soluble carbohydrate measurements were analysed by analysis of

variance (ANOVA) and Tukey multiple comparison tests (Minitab 12.0 software, Minitab Inc., PA, USA).

RESULTS

Symptom development and defence gene expression following inoculation of susceptible and resistant near-isogenic barley lines with *B. graminis*

Figure 1a shows the development of visible symptoms and the extent of fungal growth following inoculation of susceptible and resistant lines of barley with *B. graminis*. On susceptible leaves, hyphae were just visible to the naked eye 3

DAI and grew to form large colonies, with sporulation occurring 5 DAI (Fig. 1a[i]). By contrast, limited hyphal development occurred on leaves of the near-isogenic barley line carrying the *Mla12* resistance gene (Fig. 1a[iii]). In this barley line, epidermal hypersensitive cell death was triggered within 24 h of inoculation. This was visualized as whole-cell UV autofluorescence due to the accumulation of phenolic compounds, as shown in Fig. 1b(i). In addition to epidermal hypersensitive cell death, a spreading mesophyll cell death developed 2 DAI, and by 5 DAI necrotic lesions were visible (Fig. 1a[iii]). In leaves of the barley line with *mlo* resistance to *B. graminis* (caused by the *mlo5* mutation) fungal growth was arrested during penetration of the cell wall. Cell-wall appositions subtending fungal appresso-

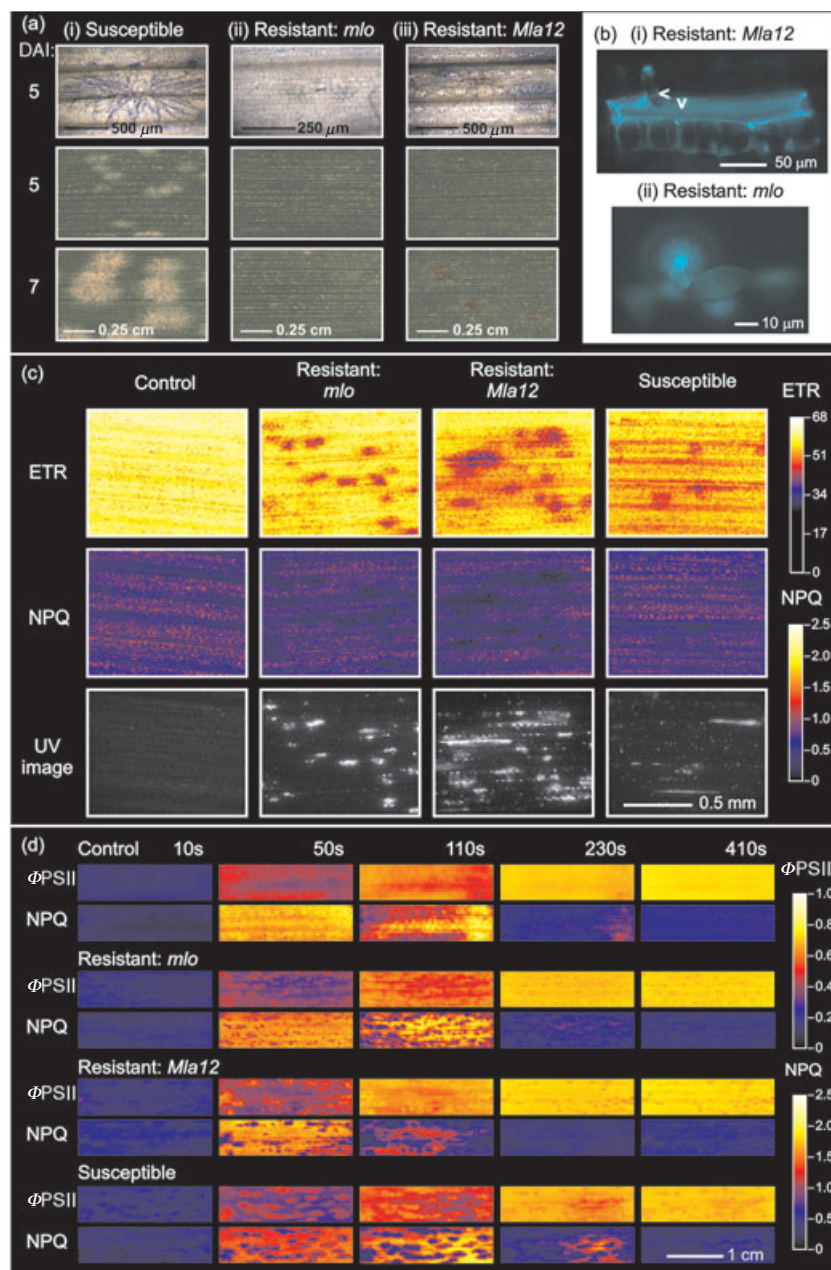


Figure 1. (a) Development of visible symptoms and fungal hyphae on barley leaves infected with *Blumeria graminis*. Top row: Fungal hyphae are stained with Brilliant Blue R. Middle row: development of visible symptoms on leaves undergoing (i) the susceptible interaction; (ii) the broad-spectrum (*mlo*) resistant interaction; and (iii) the race-specific (*Mla12*) resistant interaction, 5 days after inoculation (DAI). Bottom row: 7 DAI. (b) (i) ultraviolet (UV) autofluorescence image of an epidermal cell undergoing hypersensitive cell death as a response to pathogen challenge (*Mla12* resistance), 36 h after inoculation. Arrowheads, left: *B. graminis* conidium, down: appressorium (penetration organ). (ii) UV autofluorescence of a cell-wall apposition deposited beneath a fungal appressorium on a barley leaf undergoing a *mlo*-resistance response, 24 h after inoculation. (c) Images of the rate of photosynthetic electron transport (ETR, $\mu\text{mol m}^{-2} \text{s}^{-1}$) and non-photochemical quenching (NPQ) of a control leaf and *B. graminis*-challenged leaves, 3 DAI. Images were captured during steady-state photosynthesis at an irradiance of $200 \mu\text{mol m}^{-2} \text{s}^{-1}$. The colour scales show the relationship between colour and the relevant chlorophyll-fluorescence measurement. Corresponding greyscale images of UV autofluorescence are also shown. (d) Images of NPQ and the proportion of light flowing through photosystem II (ΦPSII) of control and infected leaves captured during the induction of photosynthesis, 5 DAI. Time after the commencement of actinic illumination ($80 \mu\text{mol m}^{-2} \text{s}^{-1}$) is indicated in seconds (s).

ria were clearly visible at this stage (Fig. 1b[ii]). However, some mesophyll damage was also evident in these leaves, with small regions of chlorosis detected 2 DAI. These regions grew slowly and remained more localized when compared to those observed on leaves carrying *Mla12*. By 5–7 DAI, lesions were only just visible to the naked eye as necrotic/chlorotic flecks on the leaf (Fig. 1a[ii]).

The expression of genes encoding PR-1, PAL and peroxidase was measured quantitatively using RT PCR. In leaves undergoing both *mlo*- and *Mla12*-mediated resistance, *PR-1* gene expression was induced 100-fold by 2 DAI and this had increased to 400-fold by 3 DAI when compared to control leaves (Fig. 2a). In infected susceptible leaves, induction of *PR-1* gene expression occurred later in the infection cycle (3 DAI) (Fig. 2a). *PAL*- and peroxidase-gene expression were not induced in control or resistant leaves during the time course studied (Fig. 2b,c). However, in susceptible leaves, peroxidase-transcript levels increased 3 DAI, and by 7 DAI, they were approximately 8-fold higher than in control leaves (Fig. 2c).

The effect of *B. graminis* on photosynthesis in susceptible and resistant barley lines

Three days after inoculation, there was no significant difference in the rate of CO₂ assimilation between control (uninfected), resistant or susceptible barley leaves at any irradiance (Fig. 3a). Five DAI, the rate of CO₂ assimilation was lower in infected susceptible leaves when compared to uninfected leaves at 200 and 400 $\mu\text{mol m}^{-2} \text{s}^{-1}$, and by 7 DAI, it was approximately 60% of control leaves at all irradiances studied (Fig. 3b,c). The rate of photosynthesis in both resistant barley lines was lower than that of control leaves at irradiances of 200 and 400 $\mu\text{mol m}^{-2} \text{s}^{-1}$ (5 DAI), and by 7 DAI this effect was greater, with CO₂ assimilation being intermediate between those of control and susceptible leaves at each irradiance studied (Fig. 3b,c).

In addition to measurements of CO₂ assimilation, images of chlorophyll fluorescence were captured during steady-state photosynthesis 3, 5 and 7 DAI and used to calculate images of ΦPSII , ETR and NPQ. Figure 1c shows representative images of ETR and NPQ 3 DAI (obtained at an irradiance of 200 $\mu\text{mol m}^{-2} \text{s}^{-1}$). Although symptoms on the leaves were barely visible at this stage, both ETR and NPQ were lower in the centres of developing lesions or colonies and in cells immediately surrounding the lesion/colony in both the susceptible and resistant interactions (Figs 1c & 4). Corresponding UV autofluorescence images showed that phenolic compounds had accumulated in and around developing lesions of both *Mla12* and *mlo* resistance (Fig. 1c).

In a leaf undergoing a compatible interaction, the mean ETR was progressively reduced in cells immediately beneath a developing colony such that by 7 DAI it was ~ 50% that of control leaves (Fig. 4b; Table 2). In regions of cells immediately adjacent to the colony, mean ETR was approximately 78% that of control leaves at 7 DAI (Fig. 4c; Table 2) but in regions of the leaf remote from the fungal

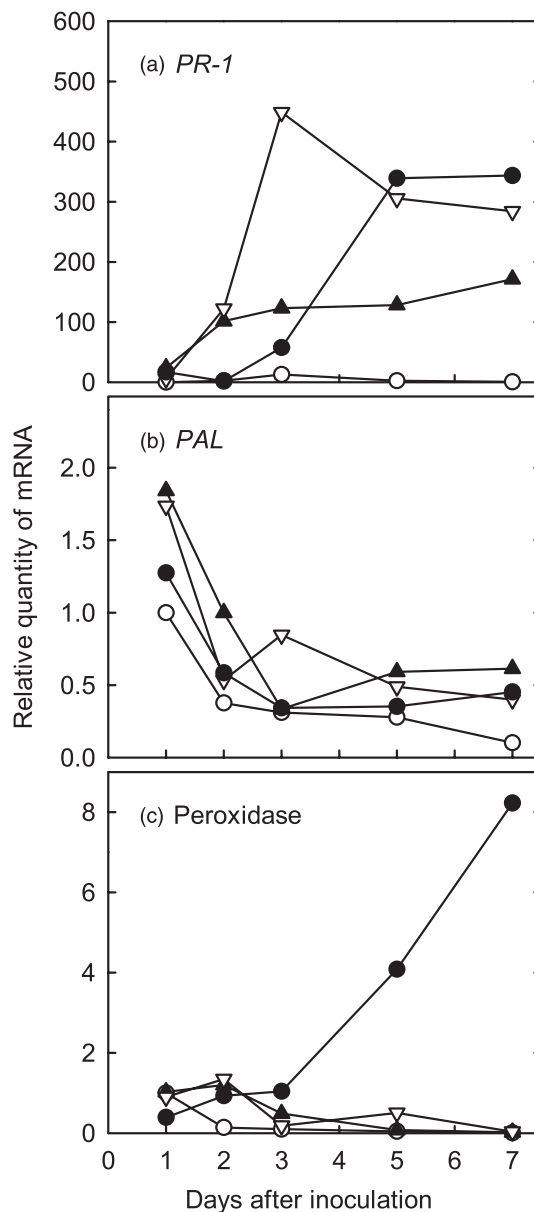


Figure 2. The expression of genes encoding defence-related proteins in control and infected leaves. The amounts of mRNA for (a) pathogenesis-related protein 1 (*PR-1*) and (b) phenylalanine ammonia lyase (*PAL*) and (c) peroxidase were determined using quantitative RT PCR. Amounts were normalized to a reference gene and were calculated relative to a control sample taken at the beginning of the experiment (day 1 timepoint). Data shown are from a representative of two independent RT PCR experiments: control leaves (○); resistant, broad-spectrum (*mlo*, ▲); resistant, race-specific (*Mla12*, ▽); susceptible (●).

colonies, the ETR was only slightly lower than that of control leaves (Fig. 4d; Table 2). By measuring the percentage of the total barley leaf occupied by each cell type, an integrated ETR (for an average-size barley leaf of 10 cm²) was calculated. This showed that in a susceptible leaf, the cells at the centre of a lesion contributed only 0.91 nmol s⁻¹ (2.6%) of the total whole-leaf ETR whilst cells adjacent to

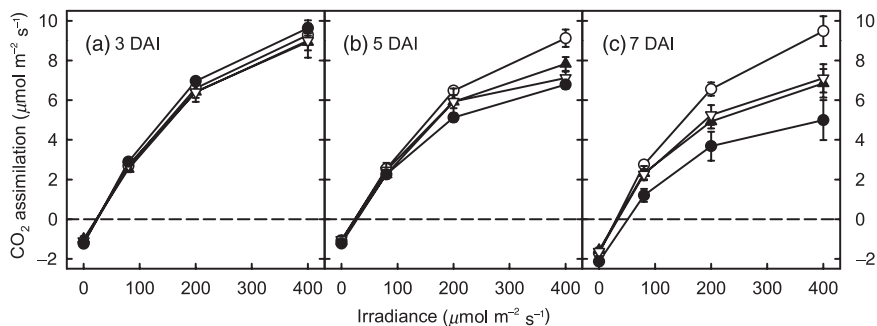


Figure 3. The effect of *Blumeria graminis* on the rate of CO₂ assimilation of barley leaves (a) 3, (b) 5 and (c) 7 days after inoculation (DAI), as measured by infrared (IR) gas analysis. Values are means \pm SE of four replicates: control (○); resistant, broad-spectrum (*mlo*, ▲); resistant, race-specific (*Mla12*, ▽); susceptible (●).

and remote from the colony contributed 16.60 and 20.10 nmol s⁻¹ (47.4 and 57.4%), respectively.

In leaves undergoing resistance responses, the mean ETR was reduced beneath sites of pathogen challenge as these cells became chlorotic/necrotic (Figs 1c & 4b). In leaves undergoing a *Mla12*-resistant interaction, a 37 and 15% drop in mean ETR was detected in cells within developing lesions and in adjacent areas by 7 DAI, respectively, when compared to the ETR of a control leaf (Table 2, Fig. 4b,c). The different cell types occupied ~2.5 and 30.0% of the total leaf area and contributed 0.75 and 11.7 nmol s⁻¹ of the total ETR of the leaf, respectively (Table 2). The remaining cells contributed 30.4 nmol (71.5%) of the ETR of leaf (Table 2). In leaves undergoing a *mlo*-resistance reaction, the chlorotic flecks covered ~7.0% of the leaf and contributed 2.6 nmol s⁻¹ of the ETR of the leaf. Cells immediately adjacent to the flecks (approximately 14% of the leaf) contributed 6.23 nmol s⁻¹ whilst the remainder of the leaf contributed 35.50 nmol s⁻¹ (Table 2).

The effects of pathogen infection on NPQ during steady-state photosynthesis are shown in Figs 1c and 4(e-h). Whole-leaf NPQ was similar in control and infected leaves 3 DAI, but from 5 DAI, the NPQ was significantly lower in all leaves challenged with *B. graminis*, when compared to control leaves (Fig. 4e; $P < 0.05$). This lowering of NPQ was most evident in cells subtending fungal colonies in a compatible interaction, or immediately below the attempted penetration site in leaves undergoing the resistant interactions (Figs 1c & 4f). A lower NPQ was also evident in cells adjacent to penetration sites (Figs 1c & 4g), and it was apparent to a lesser extent in regions remote from the pathogen challenge (Figs 1c & 4h).

The effects of *B. graminis* infection on host photosynthesis during photosynthetic induction

Images of chlorophyll fluorescence were captured during the induction of photosynthesis (at an irradiance of

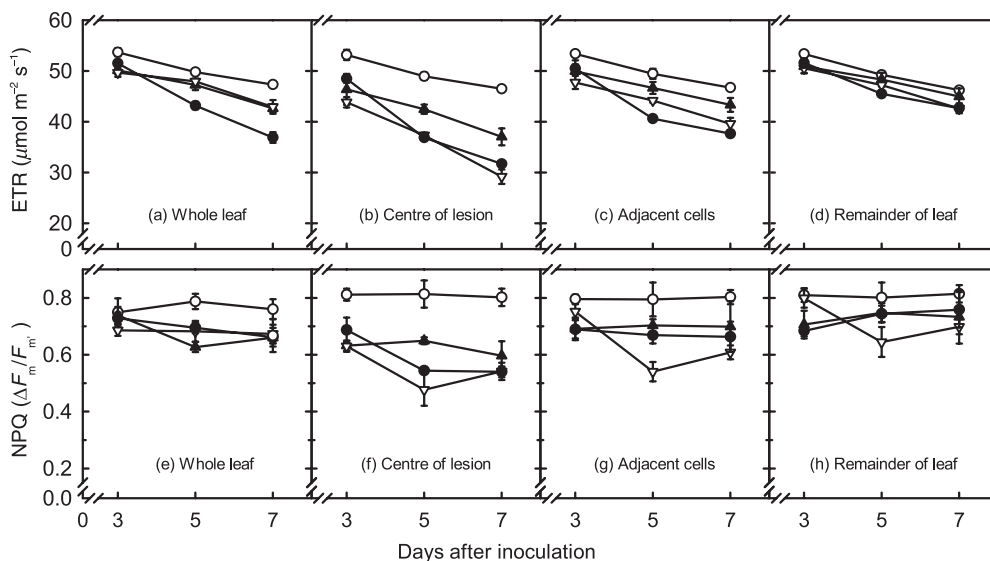


Figure 4. The effect of *Blumeria graminis* on the rate of photosynthetic electron transport (ETR) and non-photochemical quenching (NPQ) of control and infected leaves during steady-state photosynthesis at an irradiance of 200 $\mu\text{mol m}^{-2} \text{s}^{-1}$. Values for whole leaves (a, e). Centre of developing lesions (resistant interactions) or fungal colonies (susceptible interaction) (b, f). Cells immediately adjacent to developing lesions/fungal colonies (c, g). Remainder of leaf (d, h; >3 mm from pathogen challenge). Values are means \pm SE of four leaves: control (○); resistant, broad-spectrum (*mlo*, ▲); resistant, race-specific (*Mla12*, ▽); susceptible (●).

Table 2. Integrated ETR (nmol 10 cm⁻² s⁻¹) for a susceptible barley leaf or a leaf undergoing race-specific (*Mla12*) or broad-spectrum resistance (*mlo*) following infection with *Blumeria graminis* for 7 d.

Treatment	% of total leaf area occupied	Mean ETR (μmol m ⁻² s ⁻¹)	Integrated ETR (nmol 10 cm ⁻² leaf s ⁻¹)	% ETR contributed by each region of the leaf
Uninfected leaf	100.0	48.00 ± 0.23	48.00 ± 0.23	–
Susceptible leaf				
Centre of lesion	4.0 ± 1.0	22.80 ± 1.70	0.91 ± 0.00	2.6
Adjacent cells	44.9 ± 3.7	32.50 ± 1.50	14.60 ± 1.70	47.4
Remainder of leaf	50.9 ± 4.0	40.30 ± 1.40	20.10 ± 0.70	57.4
Whole leaf	100.0	34.90 ± 1.70	34.90 ± 1.70	100.0
<i>Mla12</i>				
Centre of lesion	2.5 ± 1.5	30.40 ± 1.40	0.75 ± 0.00	17.6
Adjacent cells	29.7 ± 4.8	39.70 ± 0.90	11.70 ± 0.20	33.4
Remainder of leaf	67.7 ± 12.6	45.00 ± 0.80	30.40 ± 0.50	71.5
Whole leaf	100.0	42.50 ± 0.90	42.50 ± 0.90	100.0
<i>mlo</i>				
Centre of lesion	7.0 ± 2.0	37.40 ± 1.70	2.61 ± 0.03	6.1
Adjacent cells	14.4 ± 3.9	43.30 ± 1.40	6.20 ± 0.50	14.7
Remainder of leaf	78.2 ± 2.6	44.90 ± 1.60	35.10 ± 0.04	82.9
Whole leaf	100.0	42.30 ± 1.00	42.30 ± 1.03	100.0

Photosynthesis was measured at 200 μmol m⁻² s⁻¹; values are means ± SE of 6 leaves. ETR, rate of photosynthetic electron transport.

80 μmol m⁻² s⁻¹), and the values of ΦPSII and NPQ were calculated. Figure 1d shows representative images of ΦPSII and NPQ, and Fig. 5 shows values extracted from different regions of the leaves 5 DAI. Similar results were obtained for 3 and 7 DAI (data not shown). Upon illumination of a dark-adapted control leaf, ΦPSII increased, reaching a steady-state value of 0.72 by ~ 500 s (Figs 1d & 5a,c,e). The kinetics of photosynthetic induction in infected leaves again revealed spatial heterogeneity. In regions of cells beneath fungal colonies (in a susceptible interaction) or within developing lesions (in leaves undergoing resistance responses), ΦPSII increased more rapidly after illumination than in uninfected regions of the infected leaf, or in a control leaf, reaching a slightly lower steady-state value sooner (~ 200–300 s; Fig. 5a). This effect also extended to cells adjacent to these regions, most markedly in leaves undergoing the *Mla12*-resistant interaction (Fig. 5c). Regions distant from pathogen challenge had similar patterns of ΦPSII induction to a control leaf.

Upon illumination of a dark-adapted control leaf, there was a rapid rise in NPQ that lasted for up to 100 s, after which it decreased to a low, steady-state value of ~ 0.5 (Figs 1d & 5f). In regions beneath fungal colonies or within developing lesions, there was a smaller initial peak in NPQ when compared to that seen in a control leaf (Figs 1d & 5b). This was particularly apparent in leaves undergoing a susceptible or *Mla12*-resistant interaction where the effect extended to cells adjacent to the fungal penetration site (Fig. 5d). In regions of infected leaves remote from the pathogen challenge, the kinetics of NPQ induction were similar to that of a control leaf (Fig. 5f).

The expression of genes encoding photosynthetic proteins

To measure the expression of genes encoding *rbcS* and *cab*, mRNA was quantified using RT PCR. The amount of *rbcS* mRNA was similar in control leaves and those infected with *B. graminis* (susceptible and resistant interactions) until approximately 5 DAI. Thereafter, there was a large decline in *rbcS* transcript in leaves undergoing the compatible interaction (an 80-fold reduction) and a 20-fold decline in leaves undergoing the *Mla12*-resistance reaction (Fig. 6a). The amount of *cab* mRNA followed essentially the same pattern as that of *rbcS* except that the decline started earlier (3 DAI) and also evident in leaves undergoing the *mlo*-resistance interaction (Fig. 6b).

Soluble carbohydrate content and sucrolytic enzyme activities in susceptible and resistant barley leaves infected with *B. graminis*

Figure 7 shows the amounts of hexoses and sucrose, the activities of apoplastic and soluble invertases and SS activity following inoculation with *B. graminis*. Total hexose content is shown as the amounts of glucose and fructose were similar in magnitude. The activities of all sucrolytic enzymes were low in uninfected leaves throughout the time course of the experiment and these were correlated with low amounts of hexose sugars in the leaves (Fig. 7). The amount of sucrose was approximately 0.5–1.0 mmol m⁻² in the morning reaching to 2.0–3.0 mmol m⁻² in the afternoon throughout the period of the experiment, resulting in a net accumulation of ~ 0.5–1.0 mmol m⁻² (Figs 7 & 8).

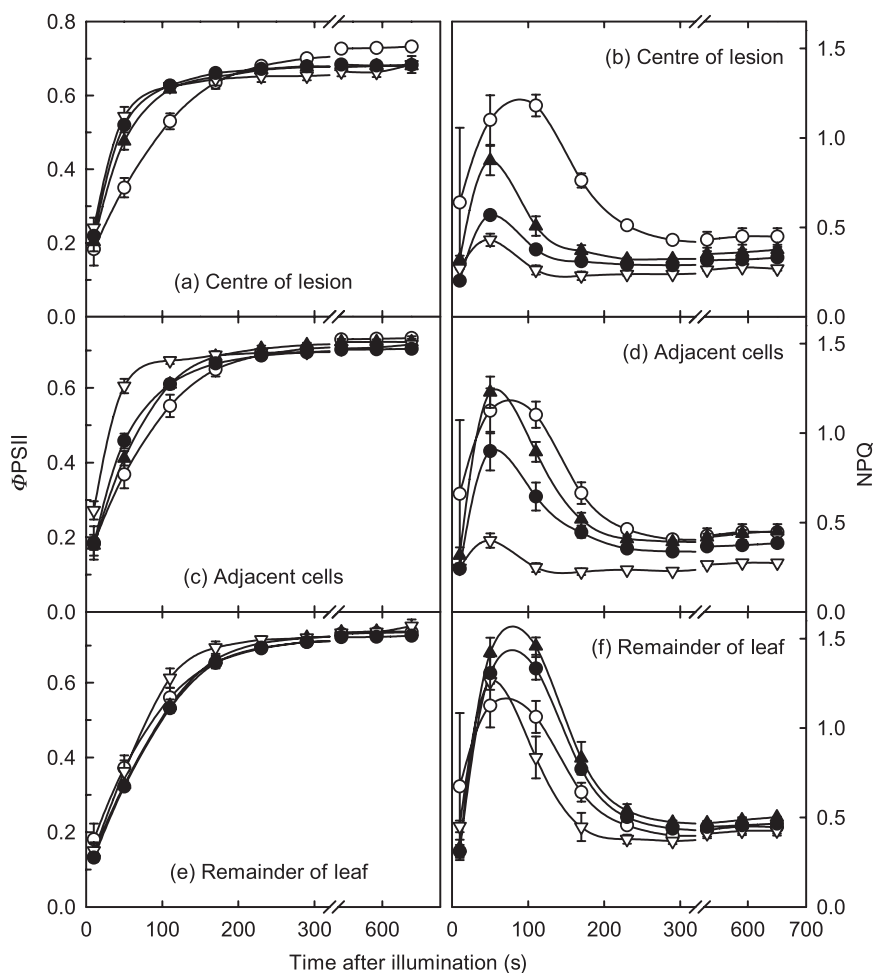


Figure 5. The effect of *Blumeria graminis* on the proportion of light flowing through photosystem II (Φ PSII) and non-photochemical quenching (NPQ) in different regions of barley leaves during the induction of photosynthesis, 5 days after inoculation (DAI) at an irradiance of $80 \mu\text{mol m}^{-2} \text{s}^{-1}$. Centre of developing lesions (resistant interactions) or fungal colonies (susceptible interaction) (a, b). Cells immediately adjacent to developing lesions/fungal colonies (c, d). Remainder of leaf (e, f; > 3 mm from pathogen challenge). Values are means \pm SE of three leaves; control (○); resistant, broad-spectrum (*mlo*, ▲); resistant, race-specific (*Mla12*, ▽); susceptible (●).

In susceptible leaves, there was a progressive and significant increase in the amount of hexoses as infection progressed (ANOVA, $P < 0.05$) such that by 7 DAI, it was eight times higher than that of control leaves (Fig. 7a). From 5 DAI, the amount of hexoses in infected leaves was significantly higher than in control leaves both in the morning (approximately 2.0 mmol m^{-2}) and evening ($3.0\text{--}4.0 \text{ mmol m}^{-2}$), resulting in a net accumulation of $1.0\text{--}1.5 \text{ mmol m}^{-2}$ hexoses (Fig. 8). The accumulation of hexose sugars was accompanied by an increase in apoplastic invertase activity such that by 7 DAI, it was 2.5-fold higher than in uninfected leaves (Fig. 7a). The amount of hexoses also increased significantly in leaves undergoing resistant interactions, reaching double the amount in control leaves 3 DAI (Tukey multiple comparison test $P < 0.05$; Fig. 7a). The amount of hexoses then remained at $\sim 1 \text{ mmol m}^{-2}$ as the experiment progressed, which was intermediate between the amount in control and susceptible leaves. There was little evidence of significant hexose accumula-

tion during the day (Fig. 8). In leaves undergoing either the *Mla12* or *mlo*-resistant interaction, apoplastic invertase activity increased significantly from 2 DAI (Tukey test, $P < 0.05$). Activity continued to increase, such that by 7 DAI it was almost four times that of control leaves, reaching $40 \text{ nmol suc cm}^{-2} \text{ min}^{-1}$ (Fig. 7c). The amount of sucrose in leaves undergoing resistance reactions was similar to the uninfected leaf, but there was evidence of accumulation of sucrose in infected susceptible leaves 5–7 DAI (Figs 7–9). There were no differences in the starch content of leaves undergoing either susceptible or resistance responses when compared to control leaves (data not shown).

Soluble invertase activity declined with age in control leaves (Fig. 7d). Activity in infected susceptible and resistant leaves also declined during the course of the experiment, but to a lesser extent than that of control leaves, such that it was significantly higher in all infected leaves 5 and 7 DAI when compared to the control leaf (Fig. 7d; ANOVA

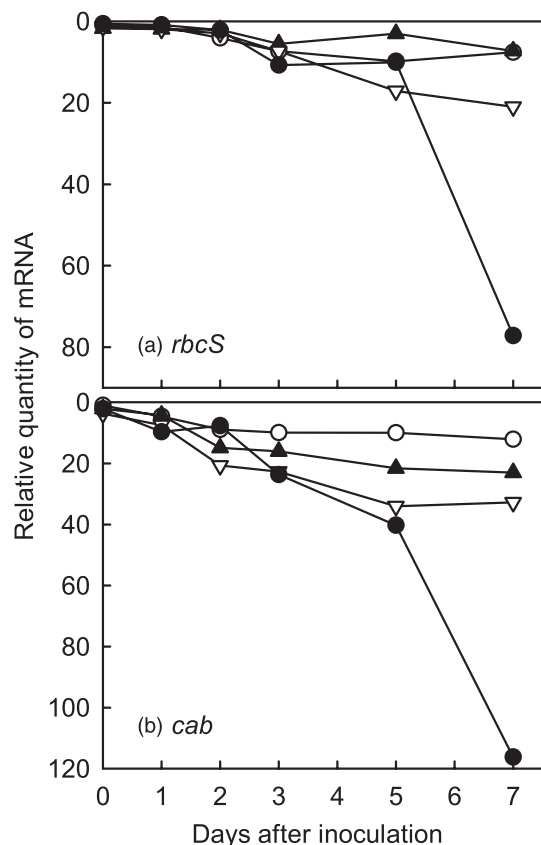


Figure 6. The expression of genes encoding photosynthetic proteins in control and infected leaves. The amounts of mRNA for (a) Rubisco (*rbcS*) and (b) chlorophyll *a/b* (*cab*) were determined using quantitative RT PCR. Amounts of *rbcS* and *cab* were normalized to a reference gene and were calculated relative to a control sample taken at the beginning of the experiment (day 1 timepoint). Data shown are from a representative of two independent RT PCR experiments: control leaves (○); resistant, broad-spectrum (*mlo*, ▲); resistant, race-specific (*Mla12*, ▽); susceptible (●).

$P < 0.05$). The activity of SS remained low during the course of the experiment, with the activity in control leaves declining from 2.4 to 1.8 $\text{nmol cm}^{-2} \text{min}^{-1}$ at 3 and 7 DAI, respectively (Fig. 7e). SS activity increased slightly in all infected leaves, such that by 7 DAI it was significantly higher than in control leaves (ANOVA, $P < 0.01$). However, SS activity was low ($\sim 2\text{--}4 \text{ nmol cm}^{-2} \text{min}^{-1}$) when compared with soluble or apoplastic invertase activities (which ranged from 10 to 50 $\text{nmol cm}^{-2} \text{min}^{-1}$).

Localization of the increase in hexose sugars, apoplastic and soluble invertase activities

Figure 9 shows the amounts of hexoses and sucrose and the activities of apoplastic and soluble invertase in the infected and unchallenged regions of infected leaves, 5 DAI. The accumulation of hexoses (Fig. 9a) and the increase in apoplastic and soluble invertase activities (Fig. 9c,d) were all localized in the infected region of the leaf in both suscep-

tible and resistant interactions. The accumulation of sucrose in the susceptible interaction was also localized to the infected region of the leaf (Fig. 9b).

DISCUSSION

How is photosynthesis affected during compatible and incompatible interactions?

In a compatible host–biotroph interaction, a reduction in the rate of whole-leaf photosynthesis is common (Farrar & Lewis 1987; Scholes 1992; Ayres *et al.* 1996), although the spatial pattern of alterations in photosynthesis varies depending upon the pathogen and host involved (Scholes & Rolfe 1996; Chou *et al.* 2000). In this study, there was also a progressive decline in the rate of photosynthesis in susceptible barley leaves infected with *B. graminis*. Quantitative imaging of chlorophyll fluorescence revealed considerable spatial and temporal heterogeneity in photosynthesis in the infected leaf; the reduction in ETR was most severe in regions of the leaf subtending the fungal colonies, but it was also substantially reduced in cells immediately adjacent to the leading edge of the mycelium. The reduction in photosynthesis in both regions contributed to the overall reduction in whole-leaf photosynthesis. Some of the reduction in ETR immediately below the colonies may have been due to a shading effect of the mycelium, although imaging of the non-challenged abaxial leaf surface still revealed a reduction in ETR beneath a large fungal colony (data not shown).

Although a reduction in photosynthesis often occurs following a compatible interaction, much less is known about the effects on photosynthesis of activating defence pathways. In both *Mla12*- and *mlo*-mediated incompatible interactions, photosynthesis was severely inhibited in cells associated with attempted penetration of the fungus. However, cells surrounding these regions also had lower ETRs and therefore contributed less to the overall rate of whole-leaf photosynthesis. These cells displayed intense autofluorescence under UV illumination indicative of the accumulation of phenolic compounds and/or callose deposition (Fig. 1c; Aist & Bushnell 1991). Thus, the depression in photosynthesis was not due only to cell death and the effective removal of green leaf area, but also to an alteration in host metabolism. The effect on ETR was more severe in leaves undergoing the *Mla12*-resistance response as the mesophyll HR associated with *Mla12*-triggered resistance continued to develop for several days after inoculation. In contrast, *mlo*-mediated immunity resulted in a more confined mesophyll cell-death response (Table 2; Hüchelhoven *et al.* 1999; Piffanelli *et al.* 2002). Zangerl *et al.* (2001) also showed both direct and indirect effects of herbivores on photosynthesis. Following caterpillar feeding in wild parsley leaves, photosynthesis was reduced when compared to an unneaten leaf due to the removal of green-leaf area. However, photosynthesis was also impaired in regions of leaf tissue surrounding damaged areas where defence-related accumulation of furanocoumarins occurred. Thus,

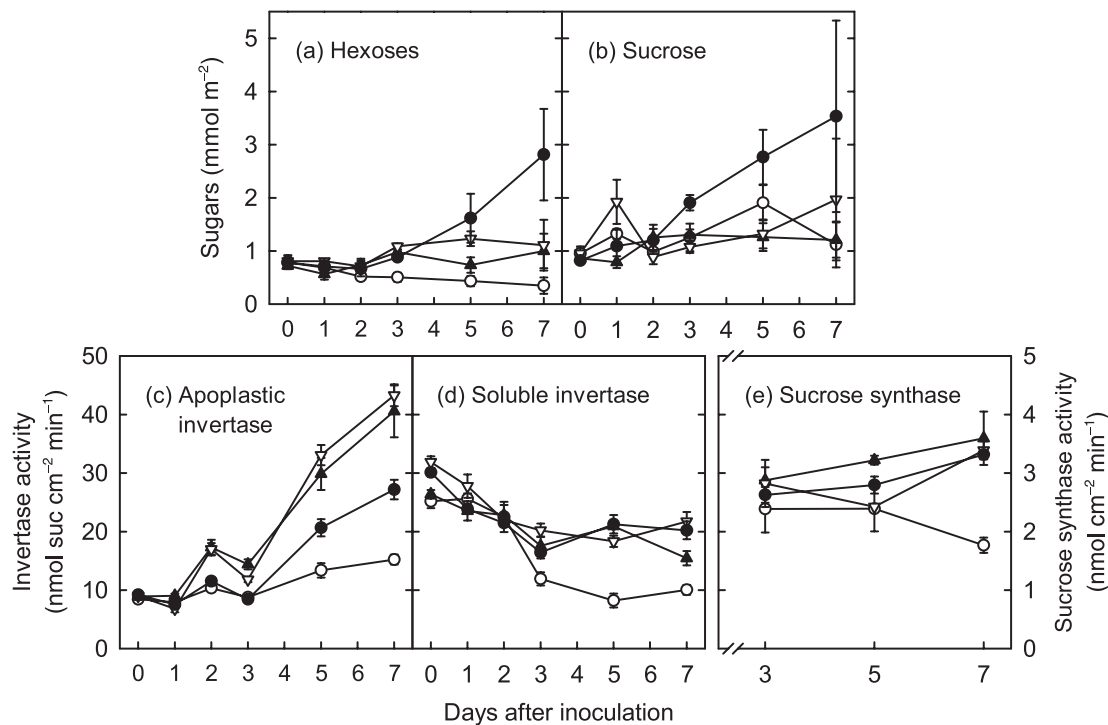


Figure 7. The effect of *Blumeria graminis* on the amounts of (a) hexoses and (b) sucrose and the activities of (c) apoplastic (cell wall-bound) invertase, (d) soluble (vacuolar) invertase and (e) sucrose synthase (SS) in barley leaves. Values are means \pm SE of four replicates: control (O); resistant, broad-spectrum (*mlo*, \blacktriangle); resistant, race-specific (*Mla12*, ∇); susceptible (\bullet).

the effects of both herbivory and the activation of resistance responses in barley leaves challenged with *B. graminis* suggest that the induction of chemical defence represents a cost to the plant in terms of carbon production and is associated with a change in carbon utilization.

An alteration in carbon/energy utilization in cells undergoing resistance reactions (particularly those adjacent to the centre of the lesion) is supported by the fact that the low values of ETR were accompanied by lower values of NPQ (for a given rate of ETR) when compared with uninfected leaves. NPQ arises from a number of processes that are induced upon exposure of leaves to light. The most important of these is high-energy-state quenching (qE), a process that depends upon the presence of the *trans*-thylakoid proton gradient (Ruban & Horton 1995; Clarke & Johnson 2001). It is possible that the lower values of NPQ resulted from the action of an uncoupler of electron transport and ATP synthesis, but there is no evidence for the production of such compounds by biotrophic fungi. It is more likely that the low values of NPQ in cells undergoing a resistance response reflect a greater metabolic demand for ATP, thus resulting in a lower *trans*-thylakoid proton gradient. An alteration in the metabolic status of these cells is also indicated by the very rapid induction of Φ PSII during a dark to light transition (Fig. 5). Meng *et al.* (2002) demonstrated that in sink regions of tobacco leaves, where carbon demand was high, induction of ETR (or Φ PSII) was very rapid. Conversely, source regions of the leaf that were

actively exporting carbon exhibited a much slower induction of Φ PSII. The *mlo*-mediated resistance response is characterized by deposition of cell-wall appositions at attempted entry sites into epidermal cells (Fig. 1b), the accumulation of defence-related transcripts (Fig. 2) and accumulation of phenolic compounds (Fig. 1b,c) (von R openack *et al.* 1998; Shirasu & Schulze-Lefert 2000; Piffanelli *et al.* 2002). *Mla12*-mediated resistance is accompanied by defence-related gene expression, the production of PR proteins and the accumulation of phenolic compounds (Figs 1b,c & 2). All these processes require energy and the diversion of carbon skeletons for defence. In cells subtending and adjacent to the developing fungal colony in a susceptible interaction, values of NPQ were also lower for a given ETR and the induction of Φ PSII during a dark to light transition was faster than in control leaves. Again this is likely to reflect increased metabolic activity but, in this case, associated with the reprogramming of metabolism to aid fungal nutrition as suggested for oat leaves infected with crown rust (Scholes & Rolfe 1996) and leaves of *Abutilon striatum* infected with abutilon mosaic virus (Osmond *et al.* 1998).

How is host carbon metabolism affected during compatible and incompatible interactions?

Infection of leaves by a range of compatible biotrophic and some necrotrophic fungal pathogens is characterized by an

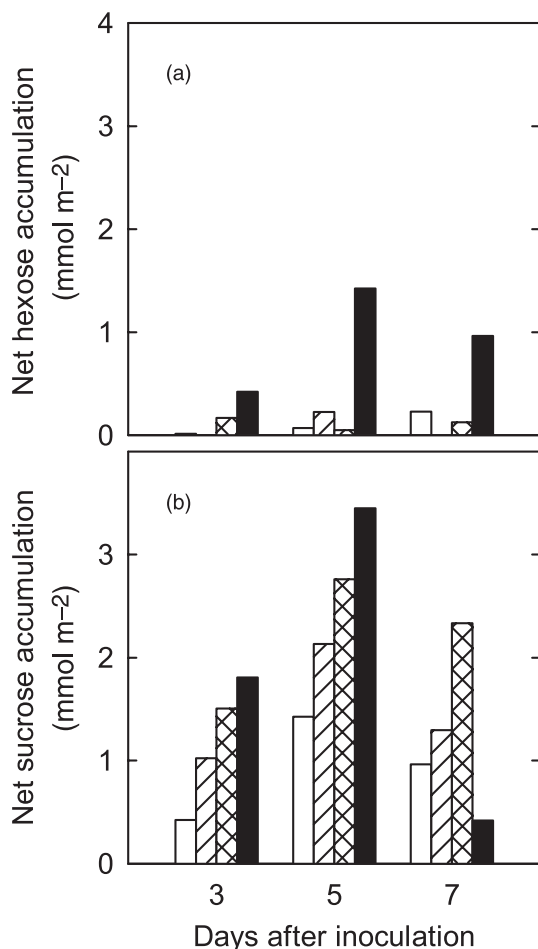


Figure 8. The net accumulation of (a) hexoses and (b) sucrose during the first 10 h of the photoperiod. Open bars, control leaves; single hatched bars, resistant broad-spectrum (*mlo*); cross-hatched bars, resistant race-specific (*Mla12*); closed bars, susceptible.

increase in host apoplastic invertase activity, an accumulation of soluble sugars and the conversion of a source leaf into a sink for carbon. This is hypothesized to aid fungal nutrition (Scholes *et al.* 1994; Chou *et al.* 2000; Hall & Williams 2000) as biotrophic fungi preferentially take up hexose sugars rather than sucrose (Voegelé *et al.* 2001; Fotopoulos *et al.* 2003). In the susceptible barley–powdery mildew interaction, an increase in invertase activity was first detectable 3–5 DAI as has been seen in other susceptible host–pathogen interactions (e.g. Tang *et al.* 1996a; Chou *et al.* 2000; Fotopoulos *et al.* 2003). The increase in invertase activity was accompanied by a progressive accumulation of hexoses and sucrose; by 5 DAI the amounts of sugars in the leaf were higher both at the end of the night and day periods when compared to control leaves. It is possible that the hydrolysis of sucrose by the elevated sacrolytic activity exceeded the capacity of the fungus to take up hexoses. It is unlikely that the increased hexose content resulted from an increase in the rate of starch or fructan breakdown during the night because both often accumulate in cereal leaves infected by powdery mildew (Zulu, Farrar & Whitbread 1991; Wright *et al.* 1995). (In

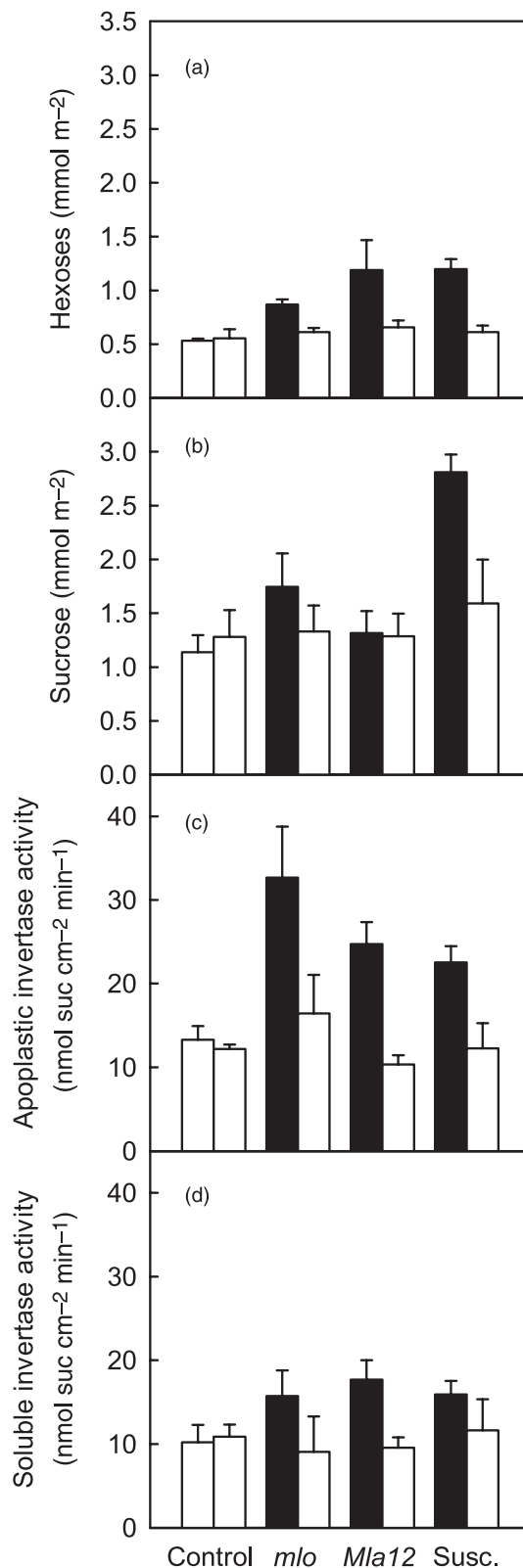


Figure 9. The effect of *Blumeria graminis* (5 days after inoculation [DAI]) on the amounts of (a) hexoses and (b) sucrose and the activities of (c) apoplastic (cell wall-bound) invertase and (d) soluble (vacuolar) invertase in infected (closed bars) and uninfected portions (open bars) of barley leaves infected only in their apical 3 cm. Values are means + SE of four replicates.

this study the starch content of infected leaves was similar to that of a control leaf). The accumulation of sucrose itself is likely to result from altered fluxes both within and into or out of the infected leaf. The metabolically active fungal mycelium represents a strong sink for carbon and an increase in import and/or a decrease in export of sucrose from infected leaves is common; interestingly, in leaves of tobacco and tomato over-expressing yeast invertase in the apoplast, both hexoses and sucrose accumulated (Dickinson, Altabella & Chrispeels 1991; Büssis *et al.* 1997). An accumulation and/or a change in flux of sugars within a leaf and across the plasma membrane can act as signals down-regulating gene expression (e.g. Koch 1996; Rolland, Moore & Sheen 2002). It has been suggested that such a mechanism may contribute to the down-regulation of *rbcs* and *cab* often seen in infected leaves (Scholes *et al.* 1994; Chou *et al.* 2000; Roitsch *et al.* 2003; Berger *et al.* 2004). In this study, photosynthetic gene expression was down-regulated on a time scale consistent with a role for sugars as signalling molecules.

An increase in invertase activity has also been implicated in disease resistance responses. Not only would a localized increase in hexoses provide energy to drive defence reactions, but sugar signals have also been shown to trigger the up-regulation of defence gene expression, for example, *PR-I* (Koch 1996; Xiao, Sheen & Jang 2000). In addition, over-expression of yeast invertase in the apoplast of tobacco plants led to the accumulation of hexoses and to the development of resistance responses such as callose deposition, cell death and the up-regulation of defence-related gene expression (Herbers *et al.* 1996; Herbers & Sonnewald 1998; Hofius *et al.* 2001; Baumart *et al.* 2001). Such observations led Roitsch *et al.* (2003) to suggest that invertase should be considered a PR protein. Despite this, few studies have examined the changes in invertase activity and carbon metabolism during genetically defined compatible and incompatible interactions. In barley leaves, the resistance pathways activated in the *mlo*- and *Mla12*-based resistant interactions are under separate genetic controls (Peterhänsel *et al.* 1997; Panstruga & Schulze-Lefert 2002) but, in both cases, apoplastic invertase activity increased and an alteration in sugar content of these leaves occurred. However, there were clear differences between the changes in carbon metabolism in the susceptible and resistant interactions. In both *mlo*- and *Mla12*-mediated resistance reactions, invertase activity increased more rapidly (detected within 48 h of inoculation) and to a greater extent than observed in infected susceptible leaves. This rapid induction of invertase activity is similar to that seen in tomato roots undergoing a resistant interaction with the necrotrophic fungal pathogen *Fusarium oxysporum* (Benhamou *et al.* 1991): invertase protein was elevated by 48 h following inoculation, compared to 3 d in the susceptible interaction. The increase in invertase activity in resistant barley leaves was not transient; activity remained high throughout the 7 d following inoculation. High invertase activity was localized to regions of cells actively undergoing resistance responses; in areas of the leaf remote from these cells, invertase activ-

ity was similar to that in a control leaf (the increase in activity was not systemic). The difference in timing of induction of invertase activity in resistant and susceptible barley leaves is in keeping with the idea that different signals may be responsible. Cell-wall invertase-transcript levels are up-regulated by a variety of signals including phytohormones (e.g. cytokinins and auxin), sugars, fungal elicitors and a range of abiotic stress-related stimuli (Ehness *et al.* 1997; Sinha *et al.* 2002; Roitsch *et al.* 2003; Balibrea Lara *et al.* 2004; Roitsch & González 2004). In the susceptible interaction, the increase in invertase activity was coincident with the increase in fungal biomass and is suggestive of a metabolic (sugar) or pathogen-dependent (perhaps cytokinin) signal. In the incompatible interactions the rapid induction of invertase activity is more in keeping with an elicitor-based signal.

The increase in invertase activity in barley leaves exhibiting *mlo*- or *Mla12*-based resistance was accompanied by a small accumulation of hexoses that was detectable within 48 h. The localization studies again showed that hexoses accumulated in areas of the leaf actively exhibiting resistance responses and the accumulation was higher than that measured in the whole-leaf study. There was no progressive build up of hexoses or sucrose in the leaves as seen in the susceptible interaction; at the end of the photoperiod the amounts of hexoses and sucrose were similar to that of control leaves. The change in hexose content (and probably fluxes within and between cells) is consistent with their active utilization to fuel defence reactions. The lack of build up of sucrose within the resistant leaves is likely to reflect the lack of a large fungal sink; it is unlikely that any additional sucrose would be imported into the leaves. There was a down-regulation in the expression of *rbcs* and *cab* gene expression (although to a lesser extent than in a compatible interaction). This may have been due to both cell death and/or to sugar-induced repression of gene expression. There was an up-regulation in the expression of *PR-I* coincident with the increase in invertase activity and accumulation of hexoses. This gene was up-regulated rapidly (24–48 h) following inoculation (in the compatible interaction expression was elevated but only after 3–7 d). These results are certainly consistent with a role for invertase in the generation of hexoses to supply energy for defence reactions and possibly with a role for hexoses in the induction of defence gene expression.

What are the consequences of activating defence reactions of plant growth and yield?

There is growing interest in the potential costs of activating resistance pathways on plant fitness and competitive ability in the natural environment, and on yield and product quality in crop plants (Purrington 2000; Brown 2002; Walters & Boyle 2005). It has been known for a long time that plants resistant to certain pathogens may suffer a yield penalty under conditions of high inoculum pressure. For example, Smedegaard-Petersen & Stolen (1981) examined the quantity and quality of barley grain yield following infection

with a virulent or avirulent isolate of *B. graminis*. They found the weight and protein content of grain to be reduced in plants following both susceptible and resistant interactions with *B. graminis* (although most markedly in compatible interactions). The mechanisms underlying this yield penalty were not clear, although it was assumed that activation of resistance pathways consumed energy that would otherwise have been utilized for growth and yield. In this study we have shown that, in barley leaves undergoing *Mla12*- or *mlo*-resistance responses, both carbon production (photosynthesis) and source-sink relations are altered in a manner that could lead to a reduction in the yield of the plant. The precise impact, under field conditions, will depend on a variety of biotic (e.g. inoculum pressure, age of plants, number of leaves affected) and abiotic (e.g. nutrient, light and water availability) conditions.

ACKNOWLEDGMENTS

We thank BBSRC for funding for P. J. S. and Dr Ken Shirasu of Sainsbury Laboratory, John Innes Centre, Norwich, UK, for providing the isolate of *B. graminis* used in this study.

REFERENCES

- Aist J.R. & Bushnell W.R. (1991) Invasion of plants by powdery mildew fungi, and cellular mechanisms of resistance. In *The Fungal Spore and Disease Initiation in Plants and Animals* (eds G.T. Cole & H.C. Hoch), pp. 321–345. Plenum, New York.
- Ayres P.G., Press M.C. & Spencer-Phillips P.T.N. (1996) Effects of pathogens and parasitic plants on source-sink relationships. In *Photoassimilate Distribution in Plants and Crops* (eds E. Zamski & A.A. Schaffner), pp. 479–499. Marcel Dekker, New York.
- Balibrea Lara M.E., Gonzalez Garcia M.-C., Fatima T., Ehness R., Lee T.K., Proels R., Tanner W. & Roitsch T. (2004) Extracellular invertase is an essential component of cytokinin-mediated delay of senescence. *The Plant Cell* **16**, 1276–1287.
- Baumart A., Mock H.P., Schmidt J., Herbers K., Sonnewald U. & Strack D. (2001) Patterns of phenylpropanoids in non inoculated and potato virus Y-inoculated leaves of transgenic tobacco plants expressing yeast-derived invertase. *Phytochemistry* **56**, 535–541.
- Benhamou N., Grenier J. & Chrispeels M. (1991) Accumulation of β -fructosidase in the cell walls of tomato roots following infection by a fungal wilt pathogen. *Plant Physiology* **97**, 739–750.
- Berger S., Papadopoulos M., Schreiber U., Kaiser W. & Roitsch T. (2004) Complex regulation of gene expression, photosynthesis and sugar levels by pathogen infection in tomato. *Physiologia Plantarum* **122**, 419–428.
- Brown J.K.M. (2002) Yield penalties of disease resistance in crops. *Current Opinion in Plant Biology* **5**, 339–344.
- Büschges R., Hollricher K., Panstruga R., et al. (1997) The barley *mlo* gene: a novel control element of plant pathogen resistance. *Cell* **88**, 695–705.
- Büssis D., Heineke D., Sonnewald U., Willmitzer L., Raschke K. & Heldt H.-W. (1997) Solute accumulation and decreased photosynthesis in leaves of potato plants expressing yeast-derived invertase either in the apoplast, vacuole or cytosol. *Planta* **202**, 126–136.
- Chou H.-M., Bundock N., Rolfe S.A. & Scholes J.D. (2000) Infection of *Arabidopsis thaliana* leaves with *Albugo candida* (white blister rust) causes a reprogramming of host metabolism. *Molecular Plant Pathology* **1**, 99–113.
- Clarke J.E. & Johnson G.N. (2001) In vivo temperature dependence of cyclic and pseudocyclic electron transport in barley. *Planta* **212**, 808–816.
- Dancer J., Hatzfeld W.-D. & Stitt M. (1990) Cytosolic cycles regulate the turnover of sucrose in heterotrophic cell-suspension cultures of *Chenopodium rubrum* L. *Planta* **182**, 223–231.
- Dickinson C.D., Altabella T. & Chrispeels M.J. (1991) Slow-growth phenotype of transgenic tomato expressing apoplastic invertase. *Plant Physiology* **95**, 420–425.
- Ehness R., Ecker M., Godt D.E. & Roitsch T. (1997) Glucose and stress independently regulate source and sink metabolism via signal transduction pathways involving protein phosphorylation. *The Plant Cell* **9**, 1825–1841.
- Farrar J.F. & Lewis D.H. (1987) Nutrient relations in biotrophic infections. In *Fungal Infection of Plants* (eds G.F. Pegg & P.G. Ayres), pp. 92–132. Cambridge University Press, Cambridge.
- Fotopoulos V., Gilbert M.J., Pittman J.K., Marvier A.C., Buchanan A.J., Sauer N., Hall J.L. & Williams L.E. (2003) The monosaccharide transporter gene, *AtSTP4*, and the cell-wall invertase, *Atβfruct1*, are induced in *Arabidopsis* during infection with the fungal biotroph *Erysiphe cichoracearum*. *Plant Physiology* **132**, 821–829.
- Hall J. & Williams L.E. (2000) Assimilate transport and partitioning in fungal biotrophic interactions. *Australian Journal of Plant Physiology* **27**, 549–560.
- Hammond-Kosack K.E. & Jones J.D. (1996) Resistance gene-dependent plant defense responses. *The Plant Cell* **8**, 1773–1791.
- Heisterüber D., Schulte P. & Moerschbacher B.M. (1994) Soluble carbohydrates and invertase in stem rust-infected, resistant and susceptible near-isogenic wheat leaves. *Physiological and Molecular Plant Pathology* **45**, 111–123.
- Herbers K. & Sonnewald U. (1998) Altered gene expression brought about by inter- and intracellularly formed hexoses and its possible implications for plant-pathogen interactions. *Journal of Plant Research* **111**, 323–328.
- Herbers K., Meuwly P., Frommer W.B., Métraux J.P. & Sonnewald U. (1996) Systemic acquired resistance mediated by the ectopic expression of invertase: possible hexose sensing in the secretory pathway. *The Plant Cell* **8**, 793–803.
- Hofius D., Herbers K., Melzer M., Omid A., Tacke E., Wolf S. & Sonnewald U. (2001) Evidence for expression level-dependent modulation of carbohydrate status and viral resistance by the potato leafroll virus movement protein in transgenic tobacco plants. *Plant Journal* **28**, 529–543.
- Hückelhoven R., Fodor J., Preis C. & Kogel K.-H. (1999) Hypersensitive cell death and papilla formation in barley attacked by the powdery mildew fungus are associated with hydrogen peroxide but not with salicylic acid accumulation. *Plant Physiology* **119**, 1251–1260.
- Jorgensen J.H. (1992) Discovery, characterization and exploitation of *Mlo* powdery mildew resistance in barley. *Euphytica* **63**, 141–152.
- Jorgensen J.H. (1994) Genetics of powdery mildew resistance in barley. *Critical Reviews in Plant Sciences* **13**, 97–119.
- Koch K.E. (1996) Carbohydrate-modulated gene-expression in plants. *Annual Review of Plant Physiology and Plant Molecular Biology* **47**, 509–540.
- Kristensen B.K., Bloch H. & Rasmussen S.K. (1999) Barley coleoptile peroxidases: purification, molecular cloning, and induction by pathogens. *Plant Physiology* **120**, 501–512.
- Lee J., Parthier B. & Lobler M. (1996) Jasmonate signalling can be uncoupled from abscisic acid signalling in barley: identifica-

- tion of jasmonate-regulated transcripts which are not induced by abscisic acid. *Planta* **199**, 625–632.
- Meng Q., Siebke K., Lippert P., Baur B., Mukherjee U. & Weis E. (2002) Sink-source transition in tobacco leaves visualised using chlorophyll fluorescence imaging. *New Phytologist* **151**, 585–595.
- Muradov A., Petrasovits L., Davidson A. & Scott K.J. (1993) A cDNA clone for a pathogenesis-related protein 1 from barley. *Plant Molecular Biology* **23**, 439–442.
- Osmond C.B., Daley P.F., Badger M.R. & Luttge U. (1998) Chlorophyll fluorescence quenching during photosynthetic induction in leaves of *Abutilon striatum* dicks: infected with abutilon mosaic virus, observed with a field portable imaging system. *Botanica Acta* **111**, 390–397.
- Panstruga R. & Schulze-Lefert P. (2002) Live and let live: insights into powdery mildew disease resistance. *Molecular Plant Pathology* **3**, 495–502.
- Peltonen S. & Karjalainen R. (1995) Phenylalanine ammonia-lyase activity in barley after infection with *Bipolaris sorokiniana* or treatment with its purified xylanase. *Journal of Phytopathology* **143**, 239–245.
- Peterhänsel C., Freialdenhoven A., Kurth J., Kolsch R. & Schulze-Lefert P. (1997) Interaction analyses of genes required for resistance responses to powdery mildew in barley reveal distinct pathways leading to leaf cell death. *The Plant Cell* **9**, 1397–1409.
- Piffanelli P., Zhou F.S., Casais C., Orme J., Jarosch B., Schaffrath U., Collins N.C., Panstruga R. & Schulze-Lefert P. (2002) The barley *Mlo* modulator of defense and cell death is responsive to biotic and abiotic stress stimuli. *Plant Physiology* **129**, 1076–1085.
- Purrington C.B. (2000) Costs of resistance. *Current Opinion in Plant Biology* **3**, 305–308.
- Roitsch T. & González M.-C. (2004) Function and regulation of plant invertases: sweet sensations. *Trends in Plant Science* **9**, 606–613.
- Roitsch T., Balibrea M.E., Hofmann M., Proels R. & Sinha A.K. (2003) Extracellular invertase: key metabolic enzyme and PR protein. *Journal of Experimental Botany* **54**, 513–524.
- Rolfe S.A. & Scholes J.D. (1995) Quantitative imaging of chlorophyll fluorescence. *New Phytologist* **83**, 499–508.
- Rolfe S.A. & Scholes J.D. (2002) Extended depth-of-focus images of chlorophyll fluorescence from intact leaves. *Photosynthesis Research* **72**, 107–115.
- Rolland F., Moore B. & Sheen J. (2002) Sugar sensing and signaling in plants. *Plant Cell* **14**, S185–S205.
- von Röpenack E., Parr A. & Schulze-Lefert P. (1998) Structural analyses and dynamics of soluble and cell wall-bound phenolics in a broad spectrum resistance to the powdery mildew fungus in barley. *The Journal of Biological Chemistry* **273**, 9013–9022.
- Ruban A.V. & Horton P. (1995) Regulation of non quenching of chlorophyll fluorescence in plants. *Australian Journal of Plant Physiology* **22**, 221–230.
- Scholes J.D. (1992) Photosynthesis: cellular and tissue aspects in diseased leaves. In *Pests and Pathogens* (ed. P.G. Ayres), pp. 82–105. BIOS Scientific Publishers Limited, Oxford.
- Scholes J.D. & Rolfe S.A. (1996) Photosynthesis in localised regions of oat leaves infected with crown rust (*Puccinia coronata*): quantitative imaging of chlorophyll fluorescence. *Planta* **199**, 573–582.
- Scholes J.D., Lee P.J., Horton P. & Lewis D.H. (1994) Invertase-understanding changes in the photosynthetic and carbohydrate metabolism of barley leaves infected with powdery mildew. *New Phytologist* **126**, 213–222.
- Shirasu K. & Schulze-Lefert P. (2000) Regulators of cell death in disease resistance. *Plant Molecular Biology* **44**, 371–385.
- Sinha A.K., Römer U., Kockenberger W., Hofmann M., Elling L. & Roitsch T. (2002) Metabolizable and non-metabolizable sugars activate different signal transduction pathways in tomato. *Plant Physiology* **128**, 1480–1489.
- Smedegaard-Petersen V. & Stolen O. (1981) Effect of energy-requiring defense reactions on yield and grain quality in a powdery mildew-resistant barley cultivar. *Phytopathology* **71**, 396–399.
- Smedegaard-Petersen V. & Tolstrup K. (1985) The limiting effect of disease resistance on yield. *Annual Review of Phytopathology* **23**, 475–490.
- Sturm A. & Chrispeels M.J. (1990) cDNA cloning of carrot extracellular β -fructosidase and its expression in response to wounding and bacterial infection. *The Plant Cell* **2**, 1107–1119.
- Tang X., Rolfe S.A. & Scholes J.D. (1996a) The effect of *Albugo candida* (white blister rust) on the photosynthetic and carbohydrate metabolism of leaves of *Arabidopsis thaliana*. *Plant, Cell and Environment* **19**, 967–975.
- Tang X.W., Ruffner H.P., Scholes J.D. & Rolfe S.A. (1996b) Purification and characterisation of soluble invertases from leaves of *Arabidopsis thaliana*. *Planta* **198**, 17–23.
- Tian D., Traw M.B., Chen J.Q. & Bergelson J. (2003) Fitness costs of R-gene-mediated resistance in *Arabidopsis thaliana*. *Nature* **423**, 74–77.
- Voegelé R.T., Struck C., Hahn M. & Mendgen K. (2001) The role of haustoria in sugar supply during infection of broad bean by the rust fungus *Uromyces fabae*. *Proceedings of the National Academy of Sciences* **98**, 8133–8138.
- Walters D.R. & Boyle C. (2005) Induced resistance and allocation costs: what is the impact of pathogen challenge? *Physiological and Molecular Plant Pathology* **66**, 40–44.
- Wolter M., Hollricher K., Salamini F. & Schulze-Lefert P. (1993) The *mlo* resistance alleles to powdery mildew infection in barley trigger a developmentally controlled defence mimic phenotype. *Molecular and General Genetics* **239**, 122–128.
- Wright D.P., Baldwin B.C., Shephard M.C. & Scholes J.D. (1995) Source-sink relationships in wheat leaves infected with powdery mildew. I: alterations in carbohydrate metabolism. *Physiological and Molecular Plant Pathology* **47**, 237–253.
- Xiao W.Y., Sheen J. & Jang J.C. (2000) The role of hexokinase in plant sugar signal transduction and growth and development. *Plant Molecular Biology* **44**, 451–461.
- Zangerl A.R., Hamilton J.G., Miller T.J., Crofts A.R., Oxborough K., Berenbaum M.R. & de Lucia E.H. (2001) Impact of folivory on photosynthesis is greater than the sum of its holes. *Proceedings of the National Academy of Sciences* **99**, 1088–1091.
- Zulu J.N., Farrar J.F. & Whitbread R. (1991) Effects of phosphate supply on wheat seedlings infected with powdery mildew – carbohydrate metabolism of first leaves. *New Phytologist* **118**, 553–558.

Received May 2005; received in revised form August 2005; accepted for publication September 2005